Int. J. Heat Mass Transfer. Vol. 34, No. 8, pp. 2013–2018, 1991
Printed in Great Britain

0017-9310/91 $3.00+0.00

Reynolds shear stress and heat flux calculations in a fully developed turbulent duct flow

R. A. ANTONIA
Department of Mechanical Engineering, University of Newcastle, N.S.W. 2308, Australia

and

J. KIM
Center for Turbulence Research, NASA–Ames Research Center, Moffett Field, CA 94035, U.S.A.

(*Received* 13 *June* 1990 *and in final form* 7 *September* 1990)

Abstract—The use of a modified form of the Van Driest mixing length for a fully developed turbulent channel flow leads to mean velocity and Reynolds stress distributions that are in close agreement with data obtained either from experiments or direct numerical simulations. The calculations are then extended to a non-isothermal flow by assuming a constant turbulent Prandtl number, the value of which depends on the molecular Prandtl number. Calculated distributions of mean temperature and lateral heat flux are in reasonable agreement with the simulations. The extension of the calculations to higher Reynolds numbers provides some idea of the Reynolds number required for scaling on wall variables to apply in the inner region of the flow.

1. INTRODUCTION

OVER THE past decade or so, direct numerical simulations (DNS) have considerably extended our ability to investigate turbulent flows. As well as providing new insight into the structure of turbulence, the data base generated by these simulations can be used to calibrate experimental techniques and to test turbulence models [1, 2]. For example, the data base obtained for a fully developed turbulent channel flow [3] has been used to test various terms in the transport equations for the Reynolds stresses, turbulent kinetic energy and dissipation rates.

In the present paper, the data of ref. [3] and more recent simulations obtained in the same flow at a higher Reynolds number are used to test a simple mixing length model. Apart from their simplicity, algebraic relations for the mixing length or eddy viscosity have performed satisfactorily, at least in simple flow geometries and relatively uncomplicated boundary conditions [4–6].

Huffman and Bradshaw [7] used a modified Van Driest mixing length distribution to analyse data in several low Reynolds number turbulent wall flows. One of the main conclusions of their analysis was that the logarithmic velocity profile remains valid provided the dimensionless shear stress gradient in the inner layer $\partial\tau^+/\partial y^+$ is numerically smaller than about 10^{-3}. For larger shear stress gradients, the Kármán constant remained unchanged, the main effect being on the additive constant in the log law. For the fully developed turbulent channel flow, one of the flows considered by these authors, $\partial\tau^+/\partial y^+$, is equal to $-(h^+)^{-1}$, where h^+ is the Reynolds (or sometimes Kármán) number, so that low Reynolds number effects on the inner region mean velocity profile should disappear when $h^+ \gtrsim 10^3$. Following a comparison (Section 2) with the DNS data, mean velocity and Reynolds shear stress distributions are presented over a wide range of h^+. In Section 3, these results are extended to a slightly heated turbulent channel flow. Mean temperature and heat flux distributions are then presented over the same h^+ range, assuming that the turbulent Prandtl number is constant, the latter depending on Pr, the molecular Prandtl number.

2. MEAN VELOCITY AND REYNOLDS SHEAR STRESS

Huffman and Bradshaw [7] obtained reasonably good agreement with Patel and Head's [8] mean velocity distributions in a fully developed channel flow by using the following mixing length distribution:

$$l^+ = \kappa y^+ \left\{1-\exp\left(-\tau^{+1/2}\frac{y^+}{A^+}\right)\right\}. \qquad (1)$$

When the total shear stress is constant in the inner region, i.e. $\tau^+ = 1$ and $A^+ = 26$ expression (1), which has also been used by Patankar and Spalding [9] and Cebeci and Smith [10], becomes identical to that first proposed by Van Driest [11].

From the definition of total shear stress

$$\tau^+ = \frac{\mathrm{d}\bar{U}^+}{\mathrm{d}y^+} - \overline{u^+v^+} \qquad (2)$$

it follows that

NOMENCLATURE

A^+	normalized Van Driest damping length
c_f	skin friction coefficient, $\tau_w/\frac{1}{2}\rho\bar{U}_M^2$
C	additive constant in log law, equation (7)
h	half-width of channel
h^+	Reynolds number, hU_τ/ν
l	mixing length, defined by $-\overline{uv} = (l\,\mathrm{d}\bar{U}/\mathrm{d}y)^2$
Pr	molecular Prandtl number, ν/γ
Pr_T	turbulent Prandtl number, defined in equation (9)
Q_w	thermometric wall heat flux
Re	Reynolds number, $\bar{U}_M 2h/\nu$
T, $\bar{T}$	instantaneous and mean temperature
T_w	wall temperature
T_τ	friction temperature, Q_w/U_τ
$\bar{T}^+$	$(\bar{T}_w - \bar{T})/T_\tau$
$\bar{U}$	mean velocity in the x-direction
$\bar{U}_M$	average velocity across channel
U_τ	friction velocity, $\tau_w^{1/2}$
u, v, w	velocity fluctuations in the x-, y-, z-directions, respectively
$\overline{uv}$	kinematic Reynolds shear stress
$\overline{v\theta}$	thermometric turbulent heat flux
x, y, z	coordinates in streamwise, normal (to the wall) and spanwise directions.

Greek symbols

γ	thermal diffusivity
θ	temperature fluctuation
κ	Kármán constant ($=0.41$)
ν	kinematic viscosity
τ	kinematic total shear stress, defined in equation (2)
τ_w	kinematic wall shear stress.

Subscript

w	wall value.

Superscript

+	normalization by U_τ for velocity, T_τ for temperature and ν/U_τ for a length scale.

$$\tau^+ = \frac{\mathrm{d}\bar{U}^+}{\mathrm{d}y^+} + \left(l^+\frac{\mathrm{d}\bar{U}^+}{\mathrm{d}y^+}\right)^2 \tag{3}$$

with the solution for $\mathrm{d}\bar{U}^+/\mathrm{d}y^+$ given by

$$\frac{\mathrm{d}\bar{U}^+}{\mathrm{d}y^+} = \frac{2\tau^+}{1+(1+4l^{+2}\tau^+)^{1/2}}. \tag{4}$$

The mean velocity distribution is obtained by numerically integrating equation (4), namely

$$\bar{U}^+ = \int_0^{y^+} \frac{2\tau^+}{1+(1+4l^{+2}\tau^+)^{1/2}}\,\mathrm{d}y^+ \tag{5}$$

with the total shear stress distribution given by

$$\tau^+ = 1 - \frac{y^+}{h^+} \tag{6}$$

and the value of A^+ taken from the A^+ vs $\partial\tau^+/\partial y^+$ correlation determined in ref. [7]. This correlation is shown in Fig. 1 in the form A^+ vs h^+. The dependence of A^+ on h^+ disappears for $h^+ \gtrsim 10^3$, when A^+ is equal to about 26.

Figure 2† confirms that equation (5), with the aid of equation (6) and the correlation of Fig. 1, yields reasonable agreement with the data of ref. [8], departures between calculation and measurement tending to occur mainly near the centreline.

It should be pointed out that the limiting behaviour of equation (1) at the wall is incorrect since it yields

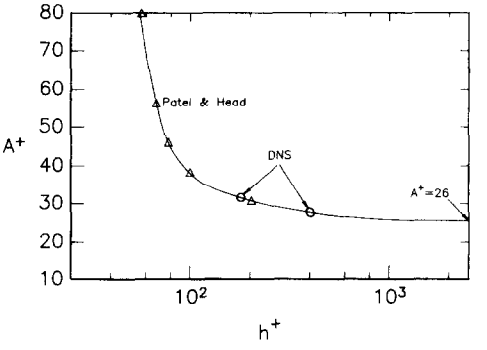

FIG. 1. Variation of the Van Driest damping length scale A^+ with Reynolds number h^+. The curve is a best fit to the fully developed channel flow data in Fig. 9 of ref. [7].

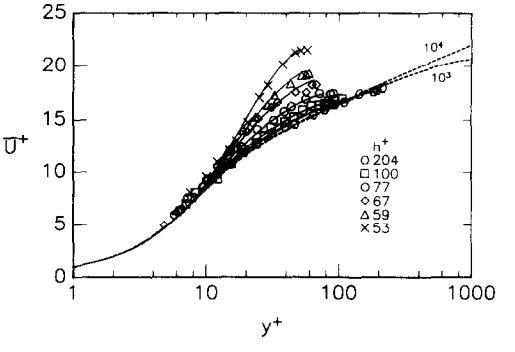

FIG. 2. Comparison with the mean velocity distributions of Patel and Head [8]. Calculations at two large values of h^+ (10^3 and 10^4) are also shown. Symbols are Patel and Head's [8] data. Curves are calculations using equation (5).

† To avoid crowding, the results for $h^+ = 125$ ($A^+ = 32$) are not shown in this figure. Results at this Reynolds number are included in subsequent figures.

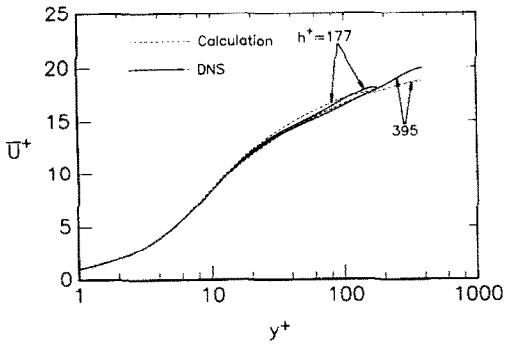

FIG. 3. Comparison with the DNS mean velocity distributions: ——, DNS; — —, calculated using equation (5).

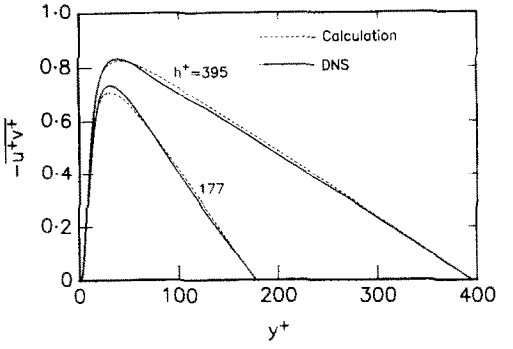

FIG. 4. Comparison with DNS Reynolds shear stress distributions: ——, DNS; — —, calculated using equations (2), (4) and (6).

$\overline{u^+v^+} \sim y^{+4}$ instead of $\overline{u^+v^+} \sim y^{+3}$. This disadvantage, which also applies to most of the mixing length or near-wall damping function distributions that have been suggested [4, 12, 13] should not be too serious in the present context where the focus is not on the near-wall region. Another difficulty is that equation (1) is unlikely to describe the flow in the duct outer region adequately when h^+ becomes large enough for the 'wake' component of velocity to become significant. The distinction between inner and outer regions becomes 'blurred' at small h^+, so that the mixing length approach will 'appear' adequate over a significant fraction of the channel.

Patel and Head [8] defined a Reynolds number Re based on the average velocity U_M and width $(2h)$ of the channel. Using their c_f vs Re correlation, the relation between h^+ and Re is given by $h^+ = 0.0686 Re^{11/12}$. Although this is the relation that was used here, a more widely applicable relation, based on the duct correlations of Dean [14], would be $h^+ = 0.955 Re^{7/8}$.

Distributions of $\bar{U}^+$ obtained for $A^+ = 26$ and $h^+ = 10^3$, 10^4 have been added to Fig. 2. They are practically indistinguishable up to $y^+ \approx 200$, and in agreement with a logarithmic distribution

$$\bar{U}^+ = \kappa^{-1} \ln y^+ + C \qquad (7)$$

($\kappa = 0.41$ and $C \approx 5$) in the range $20 \leqslant y^+ \leqslant 200$.

Direct numerical simulations of a turbulent channel flow have been carried out [3] at $h^+ \approx 177$ and more recently [15] at $h^+ = 395$. The mean velocity distributions for these simulations are compared in Fig. 3 with calculations obtained from equation (5) and the values of A^+ inferred from Fig. 1, i.e. $A^+ \approx 33$ for $h^+ = 177$ and $A^+ \approx 28$ for $h^+ = 395$. The agreement between equation (5) and the simulations is reasonable except perhaps near the centreline where the calculation underestimates the 'wake' region, especially at $h^+ \approx 395$. This deviation is not important in the context of calculating $-\overline{u^+v^+}$ from equations (2) and (6) since the magnitude of $d\bar{U}^+/dy^+$ is relatively small in the 'wake' region. Figure 4 shows that good agreement is indeed achieved between the calculated and the DNS distributions of $-\overline{u^+v^+}$.

Calculated distributions of $-\overline{u^+v^+}$ for the Patel and Head [8] values of h^+ and for $h^+ = 10^3$ and 10^4 are shown in Fig. 5. The peak magnitude of $-\overline{u^+v^+}$ continues to increase with h^+ while the y^+ location of this peak is approximately unchanged (≈ 25) for $h^+ \leqslant 100$. The peak is eventually replaced by a plateau at large enough h^+ when a constant stress region can be assumed to exist. Scaling on wall variables is clearly inappropriate for the h^+ range of Patel and Head's data in the inner region of the flow. Wei and Willmarth [16] concluded, on the basis of their measurements of $\overline{u^2}$, $\overline{v^2}$ and $-\overline{uv}$ in a turbulent channel flow, that scaling on wall variables was not satisfied over the Reynolds number range covered by their experiment ($170 \leqslant h^+ \leqslant 1600$).† Figure 5 suggests that low Reynolds number effects in the inner region are unlikely to disappear before $h^+ \approx 10^3$. The distributions for $h^+ = 10^3$ and 10^4 are quite close to each other up to $y^+ \approx 20$.

The product $-\overline{u^+v^+}\,(d\bar{U}^+/dy^+)$, the average production of turbulent kinetic energy, is shown in Fig.

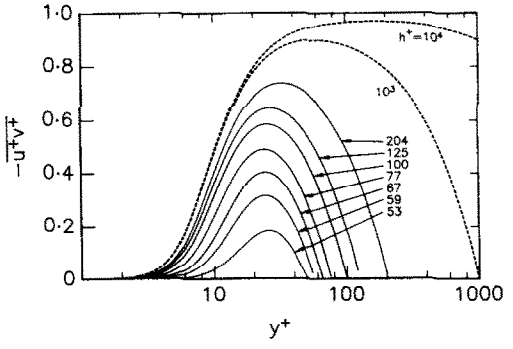

FIG. 5. Calculated distributions of Reynolds shear stress: ——, h^+ range (53–204) of ref. [8]; — —, $h^+ = 10^3$ and 10^4.

†Their measurements were actually made at $h^+ \approx 170$, 710, 990 and 1600. It is possible that Reynolds number effects have disappeared at $h^+ = 1600$ although it would be difficult to make this assertion without the benefit of data at higher h^+.

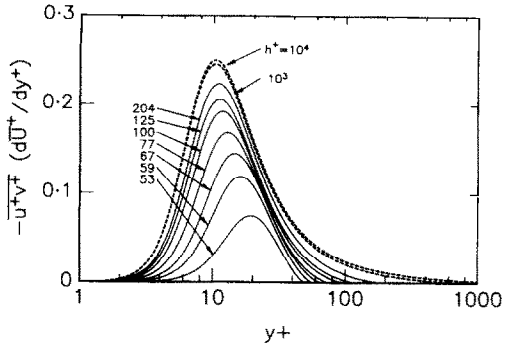

FIG. 6. Calculated distributions of average production of turbulent kinetic energy: ——, h^+ range (53–204) of ref. [8]; — —, $h^+ = 10^3$ and 10^4.

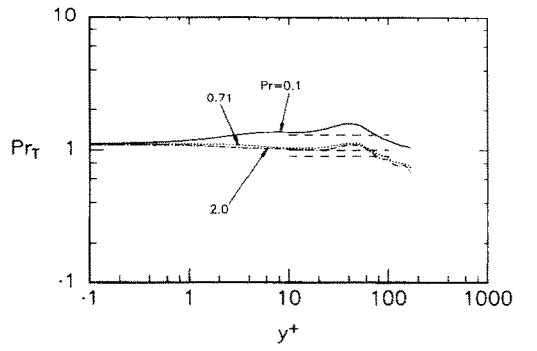

FIG. 7. Turbulent Prandtl number distributions for DNS data: ——, $Pr = 0.1$; ···, $Pr = 0.71$; —·—, $Pr = 2.0$; — —, assumed average values of Pr_T.

6. Like Fig. 5, this figure emphasizes the lack of wall scaling for the h^+ range of Patel and Head [8]. The distributions for $h^+ = 10^3$ and 10^4 are nearly coincident with a peak magnitude of about 0.25. It can be shown, using equations (2) and (6), that when $h^+ \to \infty$, the maximum value of $-\overline{u^+v^+}\ (d\bar{U}^+/dy^+)$ is 0.25 and occurs at $d\bar{U}^+/dy^+ = 0.5$.

3. MEAN TEMPERATURE AND AVERAGE HEAT FLUX

Direct numerical simulations of a non-isothermal turbulent channel flow were made in ref. [17] for $h^+ \approx 177$ and three values of the molecular Prandtl number Pr. Two types of heating conditions were used. In the first case, a passive scalar was created internally and removed from both walls while in the second, the scalar was introduced at one wall and removed at the other. Detailed statistics were presented for the first case only. For this case, the total heat flux distribution has a linear dependence on y/h, similar to equation (6)

$$q^+ = -\overline{v^+\theta^+} + \frac{1}{Pr}\frac{d\bar{T}^+}{dy^+} = 1 - \frac{y^+}{h^+} \qquad (8)$$

where $\overline{v^+\theta^+}$ and $\bar{T}^+$ are the normalized turbulent heat flux and temperature, respectively.

A simple way of determining $\overline{v^+\theta^+}$ once $\overline{u^+v^+}$ is known is to assume that the turbulent Prandtl number Pr_T, namely

$$Pr_T \equiv \frac{\overline{u^+v^+}}{\overline{v^+\theta^+}}\frac{d\bar{T}^+/dy^+}{d\bar{U}^+/dy^+} \qquad (9)$$

is constant, for a particular value of Pr. The distribution of Pr_T presented in ref. [17] and reproduced in Fig. 7 using a log–log representation have common features: a convergence towards a universal value (≈ 1.1) at the wall, a maximum at $y^+ \approx 40$ followed by a decrease toward the centreline. Here, average values of Pr_T equal to 0.9 ($Pr = 2$), 1 ($Pr = 0.71$) and 1.3 ($Pr = 0.1$) have been used (they are indicated by the horizontal lines in Fig. 7). Note that the dependence of Pr_T on Pr is qualitatively consistent with the results of Reynolds' [18] review of the relationship between Pr_T and Pr: in general, Pr_T is less than 1 when Pr is greater than 1 and vice versa. The present choices of Pr_T are also in reasonable agreement with Jischa and Rieke's [19] relation $Pr_T = c + b\,Pr^{-1}$ for $c = 0.85$ and $b = 0.05$. Strictly, b depends on Re although the dependence of Pr_T on Re is expected to be much smaller than on Pr.

The temperature gradient $d\bar{T}^+/dy^+$ can be determined from equations (8) and (9), namely

$$\frac{d\bar{T}^+}{dy^+} = \left(1 - \frac{y^+}{h^+}\right) \Big/ (Pr^{-1} + v_T^+\, Pr_T^{-1}). \qquad (10)$$

This equation can be integrated to obtain $\bar{T}^+$

$$\bar{T}^+ = \int_0^{y^+} \frac{1 - \dfrac{y^+}{h^+}}{Pr^{-1} + v_T^+\, Pr_T^{-1}}\, dy^+. \qquad (11)$$

The turbulent heat flux $-\overline{v^+\theta^+}$ is given by

$$-\overline{v^+\theta^+} = \left(1 - \frac{y^+}{h^+}\right) - Pr^{-1}\left(\frac{d\bar{T}^+}{dy^+}\right). \qquad (12)$$

The distributions of $\bar{T}^+$ and $-\overline{v^+\theta^+}$ are shown in Figs. 8 and 9, respectively. They compare favourably with the DNS results for the three values of Pr. For $\bar{T}^+$, the agreement with the DNS data is as good as that obtained using Kader's [20] formulae (Fig. 1(a)

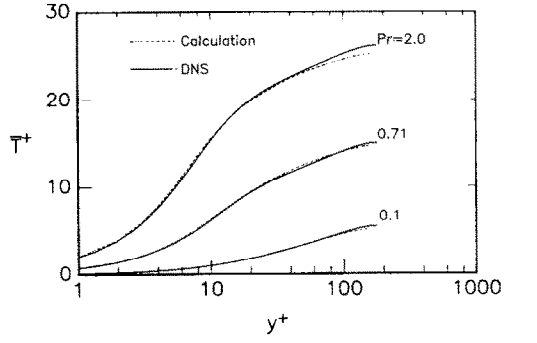

FIG. 8. Comparison between calculated mean temperature and DNS distributions: ——, DNS; — —, calculated using equation (11).

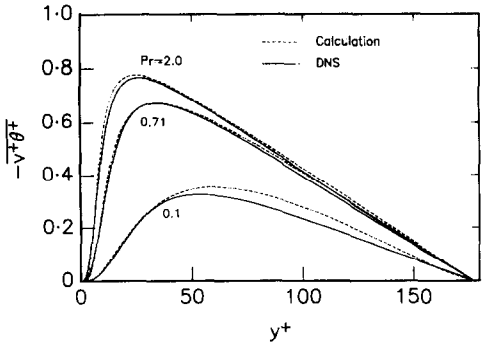

FIG. 9. Comparison between calculated heat flux and DNS distributions: ——, DNS; — —, calculated using equation (12).

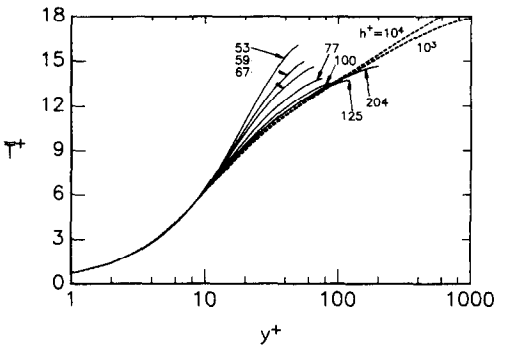

FIG. 10. Calculated mean temperature distributions: ——, h^+ range (53–204) of ref. [8]; — —, $h^+ = 10^3$ and 10^4.

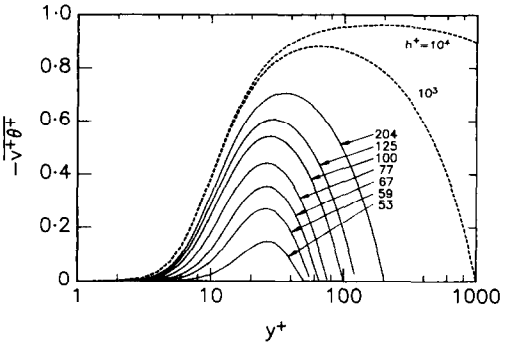

FIG. 11. Calculated heat flux distributions: ——, h^+ range (53–204) of ref. [8]; — —, $h^+ = 10^3$ and 10^4.

of ref. [17]). On the assumption that Pr_T is unaffected by h^+ (the boundary layer data of ref. [21] showed that Pr_T may be affected only at small Reynolds numbers), distributions of $\bar{T}^+$ and $-\overline{v^+\theta^+}$ were calculated using equations (11) and (12) for $Pr = 0.71$ and values of h^+ extending to 10^4. These distributions are shown in Figs. 10 and 11, respectively, while the product $-\overline{v^+\theta^+}$ $(\mathrm{d}\bar{T}^+/\mathrm{d}y^+)$, the production of the temperature variance, is shown in Fig. 12. Apart from expected differences in magnitude, these distributions exhibit similar features to those in Figs. 2, 5 and 6. Like $-\overline{u^+v^+}$, the inner regions' distributions of $-\overline{v^+\theta^+}$ do not scale on wall variables until $h^+ \approx 10^3$.

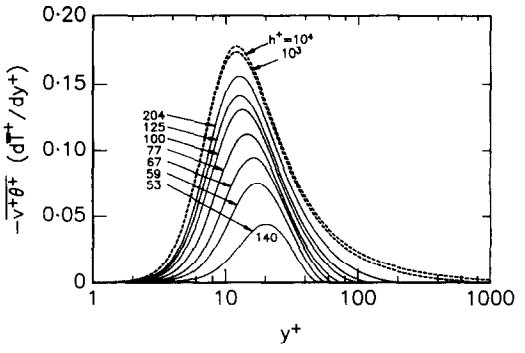

FIG. 12. Calculated distributions of the average production of temperature variance: ——, h^+ range (53–204) of ref. [8]; — —, $h^+ = 10^3$ and 10^4.

In a similar fashion to $-\overline{u^+v^+}$ $(\mathrm{d}\bar{U}^+/\mathrm{d}y^+)$, $-\overline{v^+\theta^+}$ $\times (\mathrm{d}\bar{T}^+/\mathrm{d}y^+)$ becomes approximately independent of h^+ when $h^+ \gtrsim 10^3$. When $h^+ \to \infty$, equations (2) and (12) can be used to show that the maximum value of $-\overline{v^+\theta^+}$ $(\mathrm{d}\bar{T}^+/\mathrm{d}y^+)$ is $Pr/4$ and occurs when $\mathrm{d}\bar{T}^+/\mathrm{d}y^+ = Pr/2$.

4. CONCLUSIONS AND CONCLUDING REMARKS

Use of the modified Van Driest mixing length, equation (1), leads to Reynolds shear stress distributions that are in reasonable agreement with those from direct numerical simulations of a fully developed duct flow. The assumption of a Pr-dependent turbulent Prandtl number yields adequate heat flux distributions.

With the proviso that equation (1) and the assumption of a constant turbulent Prandtl number are not too affected by the Reynolds number, the present calculations give an indication of the Reynolds number required before scaling on wall variables is satisfied in the inner region. The calculated distributions of the Reynolds shear stress and heat fluxes as well as the average productions of turbulent energy and temperature variance suggest that scaling on wall variables should apply when $h^+ \gtrsim 10^3$. This is consistent with Huffman and Bradshaw's [7] observation that low Reynolds number effects on the mean velocity in the inner region should disappear when $h^+ \gtrsim 10^3$.

It seems appropriate to conclude with some remarks about the general validity of the present choice for the mixing length distribution. This choice was suggested by the reasonable results previously obtained [7] with this distribution in this particular flow. As was noted earlier in the paper, improvements can be made to this distribution in order, for example, to yield more accurate results in the near-wall region. One could also envisage further improvements or fine tuning as more DNS data bases become available for other flows or wider ranges of Reynolds numbers. While the use of mixing length or eddy viscosity models that use wall damping functions is inevitably *ad hoc* in nature, it nevertheless represents a currently viable approach for engineering calculations.

Acknowledgements—RAA acknowledges the support of the Australian Research Council and the Center of Turbulence Research.

REFERENCES

1. N. N. Mansour, J. Kim and P. Moin, Reynolds-stress and dissipation-rate budgets in a turbulent channel flow, *J. Fluid Mech.* **194,** 15–44 (1988).
2. N. N. Mansour, J. Kim and P. Moin, Near-wall k–ε turbulence modeling, *AIAA J.* **27,** 1068–1073 (1989).
3. J. Kim, P. Moin and R. Moser, Turbulence statistics in fully developed channel flow at low Reynolds number, *J. Fluid Mech.* **177,** 133–166 (1987).
4. V. C. Patel, W. Rodi and G. Scheuerer, Turbulence models for near-wall and low Reynolds number flows: a review, *AIAA J.* **23,** 1308–1319 (1984).
5. T. Cebeci, K. C. Chang, C. Li and J. H. Whitelaw, Turbulence models for wall boundary layers, *AIAA J.* **24,** 359–360 (1986).
6. P. S. Granville, A modified Van Driest formula for the mixing length of turbulent boundary layers in pressure gradients, *J. Fluids Engng* **111,** 94–97 (1989).
7. G. D. Huffman and P. Bradshaw, A note on von Kármán's constant in low Reynolds number turbulent flows, *J. Fluid Mech.* **53,** 45–60 (1972).
8. V. C. Patel and M. R. Head, Some observations on skin friction and velocity profiles in fully developed pipe and channel flows, *J. Fluid Mech.* **38,** 181–201 (1969).
9. S. V. Patankar and D. B. Spalding, *Heat and Mass Transfer in Boundary Layers*. Morgan-Grampian, London (1967).
10. T. Cebeci and A. M. O. Smith, Report DAC, Douglas Aircraft Company (1968).
11. E. R. Van Driest, On turbulent flow near a wall, *J. Aero. Sci.* **23,** 1007–1011 (1956).
12. D. R. Chapman and G. D. Kuhn, The limiting behaviour of turbulence near a wall, *J. Fluid Mech.* **170,** 265–292 (1986).
13. P. S. Granville, A near-wall viscosity formula for turbulent boundary layers in pressure gradients suitable for momentum, heat or mass transfer, *J. Fluids Engng* **112,** 240–243 (1990).
14. R. B. Dean, Reynolds number dependence of skin friction and other bulk flow variables in two-dimensional rectangular duct flow, *J. Fluids Engng* **100,** 215–223 (1978).
15. J. Kim, On the structure of pressure fluctuations in simulated turbulent channel flow, *J. Fluid Mech.* **205,** 421–451 (1989).
16. T. Wei and W. W. Willmarth, Reynolds-number effects on the structure of a turbulent channel flow, *J. Fluid Mech.* **204,** 57–95 (1989).
17. J. Kim and P. Moin, Transport of passive scalars in a turbulent channel flow. In *Turbulent Shear Flows 6*, pp. 85–96. Springer, Berlin (1989).
18. A. J. Reynolds, The prediction of turbulent Prandtl and Schmidt numbers, *Int. J. Heat Mass Transfer* **18,** 1055–1069 (1975).
19. M. Jischa and H. B. Rieke, About the prediction of turbulent Prandtl and Schmidt numbers from modeled transport equations, *Int. J. Heat Mass Transfer* **22,** 1547–1555 (1979).
20. B. A. Kader, Temperature and concentration profiles in fully turbulent boundary layers, *Int. J. Heat Mass Transfer* **24,** 1541–1544 (1981).
21. C. S. Subramanian and R. A. Antonia, Effect of Reynolds number on a slightly heated turbulent boundary layer, *Int. J. Heat Mass Transfer* **24,** 1833–1846 (1981).

CALCUL DES TENSIONS DE REYNOLDS ET DES FLUX THERMIQUES DANS UN ECOULEMENT TURBULENT ETABLI DANS UNE CONDUITE

Résumé—L'utilisation d'une forme modifiée de la longueur de mélange de Van Driest pour les écoulements turbulents établis dans une conduite conduit à des distributions de vitesse moyenne et de tensions de Reynolds qui sont en bon accord avec les expériences ou les simulations numériques directes. Les calculs sont étendus à l'écoulement non isotherme en supposant un nombre constant de Prandtl turbulent dont la valeur dépend du nombre de Prandtl moléculaire. Les distributions calculées de température moyenne et de flux thermique latéral sont en accord raisonnable avec les simulations. L'extension des calculs aux grands nombres de Reynolds donne une idée du nombre de Reynolds utile pour la mise en échelle des variables pariétales et l'application à la région interne de l'écoulement.

BERECHNUNG DER REYNOLDS'SCHEN SCHUBSPANNUNG UND DER WÄRMESTROMDICHTE IN EINER VOLLSTÄNDIG AUSGEBILDETEN TURBULENTEN KANALSTRÖMUNG

Zusammenfassung—Mit Hilfe einer modifizierten Form der Mischungsweglänge nach van Driest wird die mittlere Geschwindigkeit und die Verteilung der Reynolds'schen Schubspannung für eine vollständig ausgebildete turbulente Kanalströmung berechnet. Die Ergebnisse stimmen gut mit solchen aus experimentellen Untersuchungen oder direkten numerischen Berechnungen überein. Das Berechnungsverfahren wird dann auf nicht isotherme Strömungen ausgedehnt, indem die turbulente Prandtl-Zahl als konstant angenommen wird—abhängig von der molekularen Prandtl-Zahl. Die berechneten Verteilungen der mittleren Temperatur und der Wärmestromdichte stimmen befriedigend mit Simulationen überein. Die Ausdehnung der Berechnungen zu größeren Reynolds-Zahlen führt zu einer Vorstellung über die Reynolds-Zahlen, die erforderlich sind, um von Wandeigenschaften auf den Kern der Strömung hochzurechnen.

РАСЧЕТЫ РЕЙНОЛЬДСОВСКОГО НАПРЯЖЕНИЯ СДВИГА И ТЕПЛОВОГО ПОТОКА В ПОЛНОСТЬЮ РАЗВИТОМ ТУРБУЛЕНТНОМ ТЕЧЕНИИ В КАНАЛЕ

Аннотация—Применение модифицированной формы длины смешения ван Дриста к полностью развитому турбулентному течению в канале позволяет определить распределение средней скорости и рейнольдсовкого напряжения, которые хорошо согласуются с данными, полученными экспериментально или при прямом численном моделировании. Затем расчеты проводятся для неизотермического течения в предположении постоянства турбулентного числа Прандтля, значение которого зависит от молекулярного числа Прандтля. Рассчитанные распределения средней температуры и поперечного теплового потока удовлетворительно согласуются с результатами моделирования. Использование расчетов для более высоких значений числа Рейнольдса дает некоторое представление о значении числа Рейнольдса, которое необходимо для того, чтобы параметры на стенке могли быть применены для расчетов во внутренней области течения.